 CMES, vol.4, no.2, pp.217-230, 2003

Finite Rotations and large Strains in Finite Element Shell Analysis

Y. Başar , O. Kintzel[1]
Institute for Structural Mechanics, Ruhr-University Bochum, Germany

Abstract: The objective of this contribution is the development of a finite element model for finite rotation and large strain analysis of thin walled shells involving geometry intersections. The shell configuration is described by a linear polynomial in the thickness coordinate. The director of the shell is multiplicatively decomposed into a stretching parameter and an inextensible unit vector whose rotation is accomplished by an updated-rotation formulation. A rotation vector with three independent components is used throughout the shell which permits advantageously to consider smooth shells and compound shells by a unified procedure. This formulation is introduced into an isoparametric four-node element. The common locking phenomena are significantly reduced by an enhancement of the strain field and the assumed strain concept.

keyword: Finite rotation, updated-rotation formulation, compound shells, large strains, enhanced strain concept

1 Introduction

In the first development phase of *finite rotation* shell elements, shell theories of KIRCHHOFF-LOVE type have been almost exclusively used for the implementation (Harte and Eckstein (1986);Nolte (1983)). A disadvantage of this approach is that the kinematic relations involve second order derivatives of the *deflection* field. This requires a relatively lengthy interpolation procedure by means of higher-order polynomials for omitting locking phenomena. To avoid this difficulty, particularly to provide an easy application of the isoparametric approach MINDLIN-REISSNER type shell formulations have been increasingly considered in the last decade in developing finite rotation shell elements. A comprehensive survey of the works achieved in this context can be found in (Başar, Itskov, and Eckstein (2000);Başar, Ding, and Schultz (1993)) .

It has been, however, later observed that the MINDLIN-REISSNER kinematics with 5 independent unknowns suffers from two significant deficiencies. The first one is that the unit length condition $\psi := \| \mathbf{d} \cdot \mathbf{d} \| - 1 = 0$ to be satisfied by the shell director $\mathbf{d}$ does not provide its unique determination during the iterative procedure. Consequently, this hypothesis is not directly applicable to finite rotation phenomena unless suitable modifications are introduced in the numerical procedure. The second deficiency occurs if geometry intersection problems are concerned. Within the MINDLIN-REISSNER hypothesis the rotation vector prescribable along the intersection lines is *tangential* to the midsurface. In dealing with two different geometries, one is therefore faced with two rotation vectors lying in two different planes. Evidently such a situation is not suitable for the *assemblage* process to be accomplished in the finite element formulation. To remove this difficulty the tangential rotation vector requires, at least along geometry intersections, an additional *twisting degree of freedom* as has been introduced e.g. in (Iura and Atluri (1992)) to develop a membrane element.

The conclusion from the above discussion is that the MINDLIN-REISSNER type shell kinematics is not capable to deal with *finite* rotations and geometry intersections. Both of the cited insufficiencies can be, however, omitted within a unified procedure by replacing the shell director by such rotational variables ensuring an a priori satisfaction of the unit length constraint.

Two different approaches have been used for this purpose in literature: determination of the director with respect to a global reference frame by means of EULER angles (Ramm (1976);Başar and Ding (1995)) or the determination of the current director by means of a rotation tensor (see e.g. Atluri (1984), Brank, Mamouri, and Ibrahimbe-

[1] Correspondence to: Ruhr-Universität Bochum, Lehrstuhl für Statik und Dynamik, Universitätsstraße 150, 44780 Bochum, Germany

gović (2003)). The rotation tensor can be parametrized by three independent variables in terms of the corresponding RODRIGUES rotation vector which leads to the so called RODRIGUES formula.

An important issue in deriving the associated tangent operator is the symmetry or nonsymmetry of the second variation (for a comprehensive review see (Suetake, Iura, and Atluri (2003),Sansour and Bufler (1992))). A well-known fact is that the second variation in vector space leads to a symmetric expression with respect to the independent variables. By utilizing the RODRIGUES formula lengthy expressions have been derived by Parisch (1991). If the corresponding relation is evaluated by considering only the incremental values of the rotation vector a symmetrical expression is obtained in any case (see Büchter and Ramm (1992)) even without an explicit parametrization of the rotation tensor in terms of the RODRIGUES rotation vector. This is a very convenient property of the so called updated rotation formulation originally proposed by (Simo and Fox (1989);Simo (1993)) particular with regard to finite element implementations. In this paper the above mentioned symmetric expression is obtained by means of a different approach solely on the basis of the calculus of variation.

The aim of this contribution is to modify MINDLIN-REISSNER kinematics such that a reliable finite element formulation for finite rotations can be achieved applicable to *smooth* and *compound* shells (Başar and Kintzel (2000)), that means to consider shells with or without geometry intersections by a unified procedure.

A further aim is the consideration of large strains, which may occur in dealing with hyperelastic materials. For this purpose transverse normal strains are included in the kinematic hypothesis by replacing the first order term in the thickness coordinate by a multiplicative decomposition $\lambda\,\mathbf{d}$ where λ describes through-the-thickness stretches (Simo, Rifai, and Fox (1990);Başar and Ding (1995)). To improve the capability of the four-node shell formulation an *enhanced assumed strain concept* is used, which renders the formulation locking-free.

2 Notations

In this paper equations are presented in tensor formulation. Variables associated with the reference configuration are denoted by upper case letters.

Points of the shell continuum are determined by position vectors, e.g. in the reference configuration :

$$\mathbf{X}=\overset{0}{\mathbf{X}}(\theta^\alpha)+\theta^3\,\overset{1}{\mathbf{X}}(\theta^\alpha),\quad \overset{1}{\mathbf{X}}=\mathbf{A}_3 \tag{1}$$

with $\mathbf{A}_3$ initially perpendicular to the midsurface. The associated geometrical elements can be evaluated by the standard procedure (Başar and Weichert (2000)) leading to :

$$\begin{aligned}&\text{Base vectors :} && \mathbf{G}_\alpha=\mathbf{A}_\alpha+\theta^3\mathbf{A}_{3,\alpha},\quad \mathbf{G}_3=\mathbf{A}_3\ ,\\ &\text{Metric tensor :} && \mathbf{G}=\mathbf{G}_i\otimes\mathbf{G}^i=G_{ij}\,\mathbf{G}^i\otimes\mathbf{G}^j\ ,\\ &\text{Determinant :} && G=|G_{ij}|\ .\end{aligned} \tag{2}$$

3 Finite rotation formulation

3.1 Basic relations

For a systematic derivation we summarize in this section some useful results (Argyris and Poterasu (1993)). The rotation of any arbitrary vector $\mathbf{D}$ into its new position $\mathbf{d}$ can be described without *singularity* by the so-called RODRIGUES *rotation vector* $\boldsymbol{\Omega}$ which describes through its direction the rotation axis and through its magnitude $\|\,\boldsymbol{\Omega}\,\|=\Omega$ the rotation angle. The corresponding relation reads as (Başar and Weichert (2000)):

$$\begin{aligned}\mathbf{d} &= \mathbf{R}(\boldsymbol{\Omega})\,\mathbf{D}\\ &= \left(\mathbf{I}+\frac{sin\,\Omega}{\Omega}\hat{\boldsymbol{\Omega}}+\frac{1-cos\,\Omega}{\Omega^2}\hat{\boldsymbol{\Omega}}\hat{\boldsymbol{\Omega}}\right)\mathbf{D}\\ &= \left(cos\,\Omega\,\mathbf{I}+\frac{sin\,\Omega}{\Omega}\hat{\boldsymbol{\Omega}}+\frac{1-cos\,\Omega}{\Omega^2}\boldsymbol{\Omega}\otimes\boldsymbol{\Omega}\right)\mathbf{D}\end{aligned} \tag{3}$$

with a rotation tensor $\mathbf{R}(\boldsymbol{\Omega})$ whose definition is given in the above relation. Herein the notation $(\,\hat{}\,)$ indicates a vector product with the successing vector.

Now attention is focused on a *skew-symmetric*, second-order tensor $\mathbf{A}=-\mathbf{A}^T$ having three independent components. The simple contraction of this tensor with an arbitrary vector $\mathbf{d}$ is expressible as

$$\mathbf{A}\,\mathbf{d}=\hat{\boldsymbol{\Omega}}\mathbf{d}=\boldsymbol{\Omega}\times\mathbf{d},\quad \hat{\boldsymbol{\Omega}}=\boldsymbol{\Omega}\times \tag{4}$$

in terms of the so-called axial vector $\boldsymbol{\Omega}$ with three independent components. The tensor function $exp\,\mathbf{A}$ can be expressed as a power-series of the form

$$exp\,\mathbf{A}=exp\,\hat{\boldsymbol{\Omega}}=\mathbf{I}+\hat{\boldsymbol{\Omega}}+\frac{1}{2!}\hat{\boldsymbol{\Omega}}^2+\frac{1}{3!}\hat{\boldsymbol{\Omega}}^3+\cdots+\frac{1}{n!}\hat{\boldsymbol{\Omega}}^n+\cdots \tag{5}$$

in terms of the axial vector $\boldsymbol{\Omega}$. It is now to be proved that the rotation vector $\boldsymbol{\Omega}$ used above is identical with that one from relation (3). Indeed, if we consider the identities

$$\hat{\boldsymbol{\Omega}}^3 = -\Omega^2 \boldsymbol{\Omega}\,, \quad \hat{\boldsymbol{\Omega}}^4 = -\Omega^2 \hat{\boldsymbol{\Omega}}^2, \; ... \tag{6}$$

expressible in a general form as

$$\begin{aligned} \hat{\boldsymbol{\Omega}}^{2n-1} &= (-1)^{n-1}\Omega^{2(n-1)}\hat{\boldsymbol{\Omega}}\,, \\ \hat{\boldsymbol{\Omega}}^{2n} &= (-1)^{n-1}\Omega^{2(n-1)}\hat{\boldsymbol{\Omega}}^2\,, \quad n = 1,2,\; ...,\; \inf \end{aligned} \tag{7}$$

equation (5) becomes

$$\begin{aligned} exp\,\hat{\boldsymbol{\Omega}} &= \mathbf{I} + \frac{1}{\Omega}\left(\Omega - \frac{\Omega^3}{3!} + \frac{\Omega^5}{5!} - ...\right)\hat{\boldsymbol{\Omega}} \\ &\quad + \frac{1}{\Omega^2}\left[1 - \left(1 - \frac{\Omega^2}{2!} + \frac{\Omega^4}{4!} - ...\right)\right]\hat{\boldsymbol{\Omega}}^2 \\ &= \mathbf{I} + \frac{sin\,\Omega}{\Omega}\hat{\boldsymbol{\Omega}} + \frac{1 - cos\,\Omega}{\Omega^2}\hat{\boldsymbol{\Omega}}\hat{\boldsymbol{\Omega}} = \mathbf{R}(\boldsymbol{\Omega})\,, \end{aligned} \tag{8}$$

demonstrating that the rotation tensor $\mathbf{R}$ defined in equation (3) in terms of the RODRIGUES rotation vector is the *closed* form of the exponential function $exp\,\hat{\boldsymbol{\Omega}}$. This connection is of significant importance for the following derivations. The above result is also discussed in further detail in Atluri and Cazzani (1995).

3.2 Updated-rotation formulation

On the basis of the identities of the previous section the relations for the updated-rotation formulation can be established by means of a solely variational procedure.

Let $\mathbf{x} = \mathbf{x}(\theta^\alpha, \theta^3)$ be the position vector of an arbitrary point of the deformed shell configuration. The basic assumption of the present development is that $\mathbf{x}$ is described by a linear expression in the thickness coordinate θ^3 :

$$\mathbf{x} = \overset{0}{\mathbf{x}}(\theta^\alpha) + \theta^3 \overset{1}{\mathbf{x}}(\theta^\alpha)\,, \quad \overset{1}{\mathbf{x}} = \lambda\,\mathbf{d} \tag{9}$$

with a multiplicative decomposition $\overset{1}{\mathbf{x}} = \lambda\,\mathbf{d}$ where $\lambda = \lambda(\theta^\alpha)$ describes through-the-thickness stretches and $\mathbf{d} = \mathbf{d}(\theta^\alpha)$ is a unit vector subjected therefore to the constraint :

$$\psi(\theta^\alpha) := \mathbf{d}\cdot\mathbf{d} - 1 = 0\,. \tag{10}$$

The above nonlinear constraint does not provide a unique determination of the director $\mathbf{d}$ during the iterative procedure. If two components of $\mathbf{d} = d^\alpha \mathbf{i}_\alpha + d^3\mathbf{i}_3$, e.g. d^α, are given, equation (10) delivers two different values $d^3 = \pm\sqrt{1 - d_\alpha d^\alpha}$ for the third one so that the convergence of the iterative procedure is not ensured for strong rotations of $\mathbf{d}$. This difficulty can be removed by replacing the director $\mathbf{d}$ by rotational quantities with which the constraint (10) is satisfied a priori. This will be achieved by the following updated formulation.

If the nonlinear variational principle $\delta\Pi = 0$ is linearized ($\Delta\delta\Pi = 0$) the director $\mathbf{d}$ is represented in it by its first variation $\delta\mathbf{d}$, the linearized form $\Delta\mathbf{d}$ as well as by $\Delta\delta\mathbf{d}$. Thus our purpose is the derivation of suitable expressions for the cited quantities providing a unique determination of $\mathbf{d}$ in each iteration step. We first introduce for $\delta\mathbf{d}$ and $\Delta\mathbf{d}$ the ansatzes :

$$\delta\mathbf{d} = \overset{V}{\boldsymbol{\omega}} \times \mathbf{d}\,, \quad \Delta\mathbf{d} = \overset{L}{\boldsymbol{\omega}} \times \mathbf{d}\,, \tag{11}$$

where $\overset{V}{\boldsymbol{\omega}}$ and $\overset{L}{\boldsymbol{\omega}}$ are additionally supposed to be arbitrary independent vectors satisfying the requirements

$$\Delta\,\overset{V}{\boldsymbol{\omega}} = \delta\,\overset{L}{\boldsymbol{\omega}} = 0\,. \tag{12}$$

It then follows for $\Delta\delta\mathbf{d}$:

$$\begin{aligned} \Delta\delta\mathbf{d} &= \overset{V}{\boldsymbol{\omega}} \times \Delta\mathbf{d} = \overset{V}{\boldsymbol{\omega}} \times (\overset{L}{\boldsymbol{\omega}} \times \mathbf{d}) \\ &= -\mathbf{d}(\overset{V}{\boldsymbol{\omega}} \cdot \overset{L}{\boldsymbol{\omega}}) + \overset{L}{\boldsymbol{\omega}}\,(\overset{V}{\boldsymbol{\omega}} \cdot \mathbf{d})\,, \end{aligned} \tag{13}$$

and similarly for $\delta\Delta\mathbf{d}$:

$$\begin{aligned} \delta\Delta\mathbf{d} &= \overset{L}{\boldsymbol{\omega}} \times \delta\mathbf{d} = \overset{L}{\boldsymbol{\omega}} \times (\overset{V}{\boldsymbol{\omega}} \times \mathbf{d}) \\ &= -\mathbf{d}(\overset{L}{\boldsymbol{\omega}} \cdot \overset{V}{\boldsymbol{\omega}}) + \overset{V}{\boldsymbol{\omega}}\,(\overset{L}{\boldsymbol{\omega}} \cdot \mathbf{d})\,. \end{aligned} \tag{14}$$

As can be deduced from the equalities

$$\Delta\delta\mathbf{d}\cdot\mathbf{d} = \delta\Delta\mathbf{d}\cdot\mathbf{d} = -\Delta\mathbf{d}\cdot\delta\mathbf{d} \tag{15}$$

obtained from (10) the order of variation δ and linearization Δ must be irrelevant in the expression $\Delta\delta\mathbf{d}$. Consequently, the variables $\overset{L}{\boldsymbol{\omega}}$ and $\overset{V}{\boldsymbol{\omega}}$ of the ansatzes (11) are in view of (13) and (14) subjected to the constraint

$$\Delta\delta\mathbf{d} = \delta\Delta\mathbf{d} = \overset{V}{\boldsymbol{\omega}} \times (\overset{L}{\boldsymbol{\omega}} \times \mathbf{d}) = \overset{L}{\boldsymbol{\omega}} \times (\overset{V}{\boldsymbol{\omega}} \times \mathbf{d}) \tag{16}$$

permitting to express $\Delta\delta\mathbf{d}$ in the form :

$$\Delta\delta\mathbf{d} = \delta\Delta\mathbf{d} = \frac{1}{2}\left(\overset{V}{\boldsymbol{\omega}} \times (\overset{L}{\boldsymbol{\omega}} \times \mathbf{d}) + \overset{L}{\boldsymbol{\omega}} \times (\overset{V}{\boldsymbol{\omega}} \times \mathbf{d})\right) \tag{17}$$

which is symmetric with respect to $\overset{L}{\boldsymbol{\omega}}$ and $\overset{V}{\boldsymbol{\omega}}$ and compatible with the requirement that the operations Δ and δ commute. It can easily be verified that the ansatzes (11) and the expression (17) deduced from it under the consideration of the requirement (15) automatically satisfy the conditions $\delta\psi = 0$ and $\Delta\delta\psi = 0$ derivable from (10). Note that the equations (11) and (17) will be used during each individual iteration step for the elimination of $\delta\mathbf{d}$, $\Delta\mathbf{d}$ and $\Delta\delta\mathbf{d}$ which automatically provides the satisfaction of the constraints $\delta\psi = \Delta\psi = \Delta\delta\psi = 0$.

In view of (17), $\overset{L}{\boldsymbol{\omega}}$ and $\overset{V}{\boldsymbol{\omega}}$ are treated as mutually interchangeable quantities so that we denote both in the following simply by $\boldsymbol{\omega}$. After evaluation of an iteration step the director $\mathbf{d}$ itself is to be constructed so as to satisfy the constraint (10) exactly. It remains to show that this can be achieved through a transformation depending on the vector $\boldsymbol{\omega}$, which will be turn out in this context to correspond to the RODRIGUES rotation vector. To derive the corresponding relation we start from (11) to form higher order terms in Δ :

$$\Delta^2\mathbf{d} = \hat{\boldsymbol{\omega}}^2\mathbf{d}\ , \quad \Delta^3\mathbf{d} = \hat{\boldsymbol{\omega}}^3\mathbf{d},\ ...,\quad \Delta^n\mathbf{d} = \hat{\boldsymbol{\omega}}^n\mathbf{d}\ . \tag{18}$$

Consequently the rotated position $\overline{\mathbf{d}}$ of $\mathbf{d}$ due to the incremental rotations $\boldsymbol{\omega}$ can be expressed by the following infinite series expansion in terms of higher order terms $\Delta^n\mathbf{d}$:

$$\begin{aligned}
\overline{\mathbf{d}} &= \mathbf{d} + \Delta\mathbf{d} + \frac{1}{2!}\Delta^2\mathbf{d} + ... + \frac{1}{n!}\Delta^n\mathbf{d} + ... \\
&= \left(\mathbf{I} + \hat{\boldsymbol{\omega}} + \frac{1}{2!}\hat{\boldsymbol{\omega}}^2 + ... + \frac{1}{n!}\hat{\boldsymbol{\omega}}^n + ...\right)\mathbf{d} \\
&= exp\,(\hat{\boldsymbol{\omega}})\,\mathbf{d} \\
&= \left(\mathbf{I} + \frac{sin\,\omega}{\omega}\,\hat{\boldsymbol{\omega}} + \frac{1-cos\,\omega}{\omega^2}\,\hat{\boldsymbol{\omega}}\hat{\boldsymbol{\omega}}\right)\mathbf{d} = \mathbf{R}\,\mathbf{d}\ .
\end{aligned} \tag{19}$$

Thus $\mathbf{d}$ is expressible in view of (8) by the rotation tensor $\mathbf{R}$ introduced in (19). We observe that the rotation vector $\boldsymbol{\omega}$ used in (11) corresponds to the RODRIGUES rotation vector describing the transformation $\mathbf{d} \rightarrow \overline{\mathbf{d}}$.

After the accomplishment of an iteration step, equation (19) will serve to determine the new position $\overline{\mathbf{d}}$ in an exact form. Starting from $\mathbf{d} = \mathbf{A}_3$, where $\mathbf{A}_3$ is the unit normal vector of the undeformed midsurface in the first iteration step, it is clear that the relation (19) provides an exact satisfaction of the constraint (10).

In the numerical procedure the vector $\boldsymbol{\omega}$ is used with components defined with respect to an orthonormal global basis $\mathbf{i}_i$:

$$\boldsymbol{\omega} = \omega^i\,\mathbf{i}_i\ , \tag{20}$$

and with components

$$\boldsymbol{\omega} = \hat{\omega}^\alpha\,\mathbf{e}_\alpha + \hat{\omega}^3\,\mathbf{d} \tag{21}$$

referring to an orthonormal local basis. Both kinds of components can be transformed into each other by

$$\hat{\omega}^k = \boldsymbol{\omega}\cdot\mathbf{e}^k = \omega^i\,(\mathbf{i}_i\cdot\mathbf{e}^k)\ . \tag{22}$$

If the decomposition (21) is used, relation (11) delivers :

$$\delta\mathbf{d} = (\hat{\omega}^\alpha\,\mathbf{e}_\alpha + \hat{\omega}^3\,\mathbf{d})\times\mathbf{d} = (\hat{\omega}^\alpha\,\mathbf{e}_\alpha)\times\mathbf{d} \tag{23}$$

showing that in this case the third component $\hat{\omega}^3$ in direction of $\mathbf{d}$ is irrelevant for the determination of $\delta\mathbf{d}$. Thus neglecting the component $\hat{\omega}^3$ transformation (17) can be replaced for this special case by

$$\Delta\delta\mathbf{d} = -\mathbf{d}\,(\boldsymbol{\omega}\cdot\boldsymbol{\omega})\ . \tag{24}$$

To construct the base vectors $\mathbf{e}_i$, needed for the decomposition (21), we make use of a rotation tensor $\overline{\mathbf{R}}$ defined as follows :

$$\begin{aligned}
\mathbf{d} &= \overline{\mathbf{R}}\,\mathbf{i}_3\ , \\
\overline{\mathbf{R}} &= (\mathbf{d}\cdot\mathbf{i}_3)\,\mathbf{I} \\
&\quad + (\mathbf{i}_3\times\mathbf{d})\times + \frac{1}{1+\mathbf{d}\cdot\mathbf{i}_3}\,(\mathbf{i}_3\times\mathbf{d})\otimes(\mathbf{i}_3\times\mathbf{d})\ , \\
\mathbf{e}_\alpha &= \overline{\mathbf{R}}\,\mathbf{i}_\alpha
\end{aligned} \tag{25}$$

transforming the global basis $\mathbf{i}_\alpha$ into $\mathbf{e}_\alpha$. Already at this stage we note that the decomposition (21) with the transformation (24) will be used at all nodes, which are not placed along geometry intersection curves and which are referred to as being regular nodes. Futher details on this are given in section 5.4.

In closing this section we recall that the director $\mathbf{d}$ is represented in the linearized principle $\Delta\delta\Pi = 0$ presented in section 4 by $\mathbf{d}$, $\Delta\mathbf{d}$, $\delta\mathbf{d}$ and $\Delta\delta\mathbf{d}$. The ansatzes (11) and (12) as well as the expression (17) deduced from it under the consideration of the requirement $\Delta\delta\mathbf{d} = \delta\Delta\mathbf{d}$ provides an exact satisfaction of the constraints $\delta\psi = \Delta\psi = 0$ and $\Delta\delta\psi = 0$ during any iteration step for arbitrary vectors $\overset{V}{\boldsymbol{\omega}}$ and $\overset{L}{\boldsymbol{\omega}}$. After the evaluation of an iteration step, the constraint $\psi = 0$ itself will be satisfied exactly trough (19). Finally the variable $\boldsymbol{\omega}$ used instead of

$\Delta\mathbf{d}$ as primary displacement quantity will be determined in the standard FE-procedure to satisfy the stationarity condition $\Delta\delta\Pi = 0$, that means, the nonlinear shell equilibrium conditions. Accordingly, the proposed approach satisfies the variational principle together with an exact enforcement of the constraint $\mathbf{d}\cdot\mathbf{d} = 1$ imposed on the director.

4 Strain measures, constitutive law

As strain measure we use the GREEN-LAGRANGE strain tensor $\mathbf{E}$ defined by

$$\mathbf{E} := E_{ij}\,\mathbf{G}^i\otimes\mathbf{G}^j = \frac{1}{2}\left(\mathbf{g}_i\cdot\mathbf{g}_j - \mathbf{G}_i\cdot\mathbf{G}_j\right)\mathbf{G}^i\otimes\mathbf{G}^j\ . \qquad (26)$$

The GREEN-LAGRANGE strains of the shell continuum have to fulfill the shell kinematics (1) and (9). By adopting these relations the deformed and undeformed base vectors of the shell continuum $\mathbf{g}_i$ and $\mathbf{G}_i$ as well as the corresponding base vectors $\mathbf{a}_i$ and $\mathbf{A}_i$ of the midsurface can be evaluated. The consideration of the shell kinematics leads to the 3D-strains given in Tab. 1.

Table 1 : $\mathbf{E}^c$ for the present kinematic assumption.

$$\begin{aligned}
E_{\alpha\beta} &= \overset{0}{E}_{\alpha\beta} + \theta^3\,\overset{1}{E}_{\alpha\beta} + (\theta^3)^2\,\overset{2}{E}_{\alpha\beta}\\
\overset{0}{E}_{\alpha\beta} &= \tfrac{1}{2}\left(\mathbf{a}_\alpha\cdot\mathbf{a}_\beta - \mathbf{A}_\alpha\cdot\mathbf{A}_\beta\right)\\
\overset{1}{E}_{\alpha\beta} &= \tfrac{1}{2}\left(\mathbf{a}_\alpha\cdot(\lambda\mathbf{d})_{,\beta} + \mathbf{a}_\beta\cdot(\lambda\mathbf{d})_{,\alpha} - \mathbf{A}_\alpha\cdot\mathbf{A}_{3,\beta} - \mathbf{A}_\beta\cdot\mathbf{A}_{3,\alpha}\right)\\
\overset{2}{E}_{\alpha\beta} &= \tfrac{1}{2}\left((\lambda\mathbf{d})_{,\alpha}\cdot(\lambda\mathbf{d})_{,\beta} - \mathbf{A}_{3,\alpha}\cdot\mathbf{A}_{3,\beta}\right)\\
E_{\alpha3} &= \overset{0}{E}_{\alpha3} + \theta^3\,\overset{1}{E}_{\alpha3}\\
\overset{0}{E}_{\alpha3} &= \tfrac{1}{2}\left(\lambda\mathbf{d}\cdot\mathbf{a}_\alpha\right)\\
\overset{1}{E}_{\alpha3} &= \tfrac{1}{2}\left(\lambda\lambda_{,\alpha}\right)\\
E_{33} &= \overset{0}{E}_{33}\\
\overset{0}{E}_{33} &= \tfrac{1}{2}\left(\lambda^2 - 1\right)
\end{aligned}$$

By using bilinear interpolation functions for the displacement field the finite element formulation suffers from several locking phenomena. However, these deficiencies can be advantageously prevented by using mixed methods. If displacements and stresses are regarded as independent quantities in the framework of the HELLINGER-REISSNER-principle (Başar, Ding, and Krätzig (1992)) a mixed hybrid formulation is obtained. On the basis of the three-field variational principle of HU-WASHIZU (Simo and Rifai (1990);Simo and Armero (1992);Betsch, Gruttmann, and Stein (1996)) the displacements, the stresses and strains, respectively, can be interpolated independently from each other. If, however, an orthogonality condition is imposed such that the stress-interpolants can be disregarded, only the displacements, leading to compatible strains, and the incompatible strains are the independent quantities in the framework of the so called *enhanced-strain*-formulation. Furthermore, it has been proved numerically (Andelfinger and Ramm (1993);Bischoff and Ramm (1997)) and theoretically (Yeo and Lee (1996)), that both methods are equivalent , if the polynomial space of the stress-interpolants related to the mixed hybrid formulation and the polynomial space of the strain-interpolants of the enhanced-strain concept form a complete bilinear polynomial space (in case of 4-noded elements). In this contribution the above mentioned enhanced-strain-formulation is used, in which additionally to the compatible strains denoted by $\mathbf{E}^c$ incompatible strains $\mathbf{E}^{inc}$ are introduced such that $\mathbf{E} = \mathbf{E}^c + \mathbf{E}^{inc}$. The HU-WASHIZU-type functional reads as follows :

$$\Pi_{HW} = \int_{\mathcal{B}} W_s\left(\mathbf{E}^c + \mathbf{E}^{inc}\right)dV - \int_{\mathcal{B}}\tilde{\mathbf{S}} : \mathbf{E}^{inc}\,dV - \Pi^{ext}_{HW}\ , \qquad (27)$$

where Π_{HW} and Π^{ext}_{HW} are the total and external potential energy, respectively. If the condition $\int_{\mathcal{B}}\tilde{\mathbf{S}} : \mathbf{E}^{inc}\,dV = 0$ is fullfilled, the stress term drops out and the functional Π_{HW} reduces to :

$$\Pi_{HW} = \int_{\mathcal{B}} W_s\left(\mathbf{E}^c + \mathbf{E}^{inc}\right)dV - \Pi^{ext}_{HW}\ . \qquad (28)$$

The related stationary condition ($\delta\Pi_{HW} = 0$) reads then as :

$$\int_{\mathcal{B}}\frac{\partial W_s}{\partial\mathbf{E}} : \delta\mathbf{E}^c\,dV + \int_{\mathcal{B}}\frac{\partial W_s}{\partial\mathbf{E}} : \delta\mathbf{E}^{inc}\,dV - \frac{\partial\Pi^{ext}_{HW}}{\partial\mathbf{u}}\cdot\delta\mathbf{u} = 0\ . \qquad (29)$$

The next step is to introduce the constitutive law. It should be mentioned that, through the inclusion of transversal normal strains, the current finite element formulation permits an easy implementation of arbitrary

three dimensional material laws. In this contribution attention is restricted to the ST. VENANT-KIRCHHOFF material with the strain energy density :

$$W_s = \frac{1}{2}\lambda\,(tr\,\mathbf{E})^2 + \mu\,tr\mathbf{E}^2 \ . \tag{30}$$

The partial derivation of the strain energy W_s with respect to the GREEN-LAGRANGE strain tensor finally leads to the 2nd PIOLA-KIRCHHOFF stress tensor :

$$\mathbf{S} = S^{ij}\mathbf{G}_i \otimes \mathbf{G}_j = \frac{\partial W_s}{\partial \mathbf{E}} = \lambda(tr\,\mathbf{E})\mathbf{G} + 2\mu\mathbf{E} \tag{31}$$

as energy conjugate quantity to $\mathbf{E}$. The linearization of (29) with respect to the compatible and incompatible strains as well the displacements is obtained as

$$\begin{aligned}&\int_{\mathcal{B}} \Delta\mathbf{E}^c : \mathbf{C} : \delta\mathbf{E}^c\,dV + \int_{\mathcal{B}} \Delta\mathbf{E}^{inc} : \mathbf{C} : \delta\mathbf{E}^c\,dV \\ &+ \int_{\mathcal{B}} \Delta\mathbf{E}^c : \mathbf{C} : \delta\mathbf{E}^{inc}\,dV + \int_{\mathcal{B}} \Delta\mathbf{E}^{inc} : \mathbf{C} : \delta\mathbf{E}^{inc}\,dV \\ &+ \int_{\mathcal{B}} \mathbf{S} : \Delta\delta\mathbf{E}^c\,dV + f_{int} - f_{ext} = 0\end{aligned} \tag{32}$$

with the unbalanced forces

$$f_{int} = \int_{\mathcal{B}} \mathbf{S} : \delta\mathbf{E}^c + \int_{\mathcal{B}} \mathbf{S} : \delta\mathbf{E}^{inc} dV \ , \tag{33}$$

the external forces f_{ext}, and with the fourth-order material tensor :

$$\mathbf{C} = \frac{\partial^2 W_s}{\partial\mathbf{E}\partial\mathbf{E}} = \lambda\,\mathbf{I}\otimes\mathbf{I} + 2\mu\ \overset{(4)}{\mathbf{I}} \ . \tag{34}$$

5 Finite element formulation

5.1 The interpolation of independent displacement variables

Starting from the incremental formulation (32) a *four-node* finite shell element is developed according to the isoparametric approach. The independent kinematic quantities entering in the assumption (1) and (9) are interpolated by means of bilinear polynomials expressible as

$$N_K = \frac{1}{4}(1+\xi_K\,\xi)(1+\eta_K\,\eta) \tag{35}$$

in terms of the natural basis $(\xi,\eta) \in \{-1,1\}$ and the coordinates ξ_K, η_K referring to the nodes. The corresponding equations read as

$$\overset{0}{\mathbf{x}} = \sum_{K=1}^{4} N_K\ \overset{0}{\mathbf{x}}{}^K \ , \quad \lambda = \sum_{K=1}^{4} N_K\,\lambda^K \ , \tag{36}$$

where index K denotes nodal values. Starting from the expressions (36) the quantitities $\delta\mathbf{a}_\alpha, \Delta\mathbf{a}_\alpha, \cdots$ can be obtained easily. Note in this context that $\Delta\delta\mathbf{a}_\alpha = \Delta\delta\lambda = 0$, since the midsurface position vector and the stretching parameter are independent quantities.

5.2 The interpolation of the shell director

Now attention is focused to the director $\mathbf{d}$, which needs in view of the constraint (10) a special treatment in the numerical procedure. In this context it is important to note that the variation $\delta\mathbf{d}$ and the linearization $\Delta\delta\mathbf{d}$ of this variable is of relevance during an iteration step. For the implementation of the considered quantities we make use of two different approaches. In the first one $\delta\mathbf{d}$ and

Table 2 : Variation of the director (Version A)

	$\delta\mathbf{d}$	$=$	$\sum_{K=1}^{4} N_K(\delta\mathbf{d}^k)$
	$\delta\mathbf{d}_{,\alpha}$	$=$	$\sum_{K=1}^{4} N_{K,\alpha}(\delta\mathbf{d}^k)$
$A1$:	$\Delta\delta\mathbf{d}$	$=$	0
	$\Delta\delta\mathbf{d}_{,\alpha}$	$=$	0
$A2$:	$\Delta\delta\mathbf{d}$	$=$	$\sum_{K=1}^{4} N_K(\Delta\delta\mathbf{d}^k)$
	$\Delta\delta\mathbf{d}_{,\alpha}$	$=$	$\sum_{K=1}^{4} N_{K,\alpha}(\Delta\delta\mathbf{d}^k)$

$\Delta\delta\mathbf{d}$ are directly interpolated similar to (36) and are then expressed in terms of the nodal rotation vector $\boldsymbol{\omega}^k$ and nodal director $\mathbf{d}^k$ according to (11) and (17) leading to :

$$\begin{aligned}\delta\mathbf{d}^k &= \boldsymbol{\omega}^K \times \mathbf{d}^K \ , \\ \Delta\delta\mathbf{d}^k &= \frac{1}{2}(\overset{V}{\boldsymbol{\omega}}{}^K \times (\overset{L}{\boldsymbol{\omega}}{}^K \times \mathbf{d}^K) + \overset{L}{\boldsymbol{\omega}}{}^K \times (\overset{V}{\boldsymbol{\omega}}{}^K \times \mathbf{d}^K)) \ .\end{aligned} \tag{37}$$

The basic relations of this approach derived from (37) are summarized in Tab. 2 and denoted as approach $A2$. On the contrary, in the second approach the transformations (11) and (17) are considered with the director $\mathbf{d}$ and the rotation vector $\boldsymbol{\omega}$ at the corresponding GAUSS-point which are interpolated according to (36). The basic relations of this alternative denoted as version B are summarized in Tab. 3. The rotation vector $\boldsymbol{\omega} = \omega^i\,\mathbf{i}_i$ is to be used with three independent components with respect to the global basis $\mathbf{i}_i$ throughout the shell. However, in case

Table 3 : Variation of the director (Version B)

$$
\begin{aligned}
\delta\mathbf{d} &= (\sum_{K=1}^{4} N_K \boldsymbol{\omega}^K)\times\mathbf{d}\\
\delta\mathbf{d}_{,\alpha} &= (\sum_{K=1}^{4} N_{K,\alpha}\boldsymbol{\omega}^K)\times\mathbf{d}+(\sum_{K=1}^{4} N_K\boldsymbol{\omega}^K)\times\mathbf{d}_{,\alpha}\\
\Delta\delta\mathbf{d} &= \frac{1}{2}((\sum_{K=1}^{4} N_K \overset{V}{\boldsymbol{\omega}}{}^K)\times((\sum_{L=1}^{4} N_L \overset{L}{\boldsymbol{\omega}}{}^L)\times\mathbf{d})\\
&\quad +(\sum_{K=1}^{4} N_K \overset{L}{\boldsymbol{\omega}}{}^K)\times((\sum_{L=1}^{4} N_L \overset{V}{\boldsymbol{\omega}}{}^L)\times\mathbf{d}))\\
\Delta\delta\mathbf{d}_{,\alpha} &= \frac{1}{2}((\sum_{K=1}^{4} N_{K,\alpha} \overset{V}{\boldsymbol{\omega}}{}^K)\times((\sum_{L=1}^{4} N_L \overset{L}{\boldsymbol{\omega}}{}^L)\times\mathbf{d})\\
&\quad +(\sum_{K=1}^{4} N_K \overset{V}{\boldsymbol{\omega}}{}^K)\times((\sum_{L=1}^{4} N_{L,\alpha} \overset{L}{\boldsymbol{\omega}}{}^L)\times\mathbf{d})\\
&\quad +(\sum_{K=1}^{4} N_K \overset{V}{\boldsymbol{\omega}}{}^K)\times((\sum_{L=1}^{4} N_L \overset{L}{\boldsymbol{\omega}}{}^L)\times\mathbf{d}_{,\alpha})\\
&\quad + \text{terms with } \overset{V}{\boldsymbol{\omega}} \text{ and } \overset{L}{\boldsymbol{\omega}} \text{ interchanged)}
\end{aligned}
$$

of smooth shells or at regular nodes of compound shells the simplification (24) can be used (see section 5.4). The director is in both cases exactly updated by using the rotation tensor $\mathbf{R}$:

$$
\begin{aligned}
&\text{Version A} \;:\; \overset{n+1}{\mathbf{d}}{}^K = \mathbf{R}\,\overset{n}{\mathbf{d}}{}^K\,, \quad \overset{n+1}{\mathbf{d}} = \sum_{K=1}^{4} N_K \overset{n+1}{\mathbf{d}}{}^K\,,\\
&\text{Version B} \;:\; \overset{n+1}{\mathbf{d}} = \mathbf{R}\,\overset{n}{\mathbf{d}}\,.
\end{aligned}
\tag{38}
$$

It then follows for the derivative of the director :

$$
\begin{aligned}
&\text{Version A} \;:\; \overset{n+1}{\mathbf{d}}_{,\alpha} = \sum_{K=1}^{4} N_{K,\alpha} \overset{n+1}{\mathbf{d}}{}^K\,,\\
&\text{Version B} \;:\; \overset{n+1}{\mathbf{d}}_{,\alpha} = \mathbf{R}_{,\alpha}\,\overset{n}{\mathbf{d}} + \mathbf{R}\,\overset{n}{\mathbf{d}}_{,\alpha}\,.
\end{aligned}
\tag{39}
$$

A detailed derivation of the above relation is given at the end of the paper. In the first iteration step we set :

$$
\overset{0}{\mathbf{d}}_{,\alpha} = \sum_{K=1}^{4} N_{K,\alpha}\mathbf{A}_3^K\,, \tag{40}
$$

where $\mathbf{A}_3$ denotes the unit normal vector of the middle surface in the reference configuration. In Version B we additionally normalize the director $\overset{0}{\mathbf{d}}$ and use the corresponding derivative instead of (40) such that the unit length condition is fullfilled a priori.

5.3 Stabilization procedure

The above described finite element formulation is subjected to various locking phenomena, namely shear, membrane and POISSON´s locking. Now our aim is to describe the stabilization algorithms used for reducing these deficiencies.

To eliminate shear locking the *natural assumed-strain concept* [Bathe and Dvorkin (1985)] is applied, where the transversal shear strains are interpolated according to

$$
\begin{aligned}
E_{13} &= \tfrac{1}{2}(1+\eta)E_{13}^A + \tfrac{1}{2}(1-\eta)E_{13}^C\,,\\
E_{23} &= \tfrac{1}{2}(1-\xi)E_{23}^B + \tfrac{1}{2}(1+\xi)E_{23}^D\,,
\end{aligned}
$$

where the superscript denotes the collocation point at which the strain components are computed, at point A ($\xi=0,\eta=1$), B ($\xi=-1,\eta=0$), C ($\xi=0,\eta=-1$) and D ($\xi=1,\eta=0$), respectively.

To reduce membrane locking the *enhanced-strain concept* is used. Within the frame of this concept the membrane strains are enriched by incompatible strains which are assumed to be of the form :

$$
\begin{bmatrix} \Xi_{11} \\ \Xi_{22} \\ 2\Xi_{12} \end{bmatrix} = \begin{bmatrix} \xi & 0 & 0 & 0 & \xi\eta & 0 & 0 \\ 0 & \eta & 0 & 0 & 0 & \xi\eta & 0 \\ 0 & 0 & \xi & \eta & 0 & 0 & \xi\eta \end{bmatrix} \cdot \begin{bmatrix} \alpha_1 \\ \alpha_2 \\ \vdots \\ \alpha_7 \end{bmatrix}. \tag{41}
$$

where $\alpha_1, \alpha_2, \cdots$ are constant parameters. Note that the rows and columns of the above matrix are linearly independent. Furthermore, the present polynomials for the incompatible strains have no counterpart in the polynomial space of the compatible strains. To satisfy the patch test the orthogonality condition $\int_{\mathcal{B}} \tilde{\mathbf{S}} : \mathbf{E}^{inc} dV = 0$ has to be fulfilled for at least constant assumed stresses $\tilde{\mathbf{S}}$, leading to the condition :

$$
\int_{\mathcal{B}} \mathbf{E}^{inc} dV = 0\,. \tag{42}
$$

To meet the above requirement, also for distorted elements, the incompatible strains (41) are to be referred to the basis of the centre point of the shell element. The incompatible strains at an arbitrary point can be obtained through the following transformation :

$$
\overset{0}{E}{}^{inc}_{\alpha\beta} = \frac{\sqrt{A_0}}{\sqrt{G}}(\mathbf{G}_\alpha\cdot\mathbf{A}_0^\rho)\,\Xi_{\rho\lambda}\,(\mathbf{A}_0^\lambda\cdot\mathbf{G}_\beta)\,, \tag{43}
$$

with index " 0 " denoting the value of a variable at the considered element centre.

For the elimination of POISSON ´s locking we enhance the constant transversal normal strain similar to (41, 43). For this case the interpolation procedure reads as (Betsch, Gruttmann, and Stein (1996)) :

$$\Xi_{33} = \left[\begin{array}{cccc} 1 & \xi & \eta & \xi\eta \end{array} \right] \left[\begin{array}{c} \alpha_8 \\ \alpha_9 \\ \alpha_{10} \\ \alpha_{11} \end{array} \right] , \tag{44}$$

$$\overset{1}{E}{}^{inc}_{33} = \frac{\sqrt{A_0}}{\sqrt{G}} \Xi_{33} . \tag{45}$$

In addition to the existing nodal degrees of freedom $\mathbf{u}_j^T$

$$\begin{gathered} \mathbf{u} = \left[\mathbf{u}_1^T \, \mathbf{u}_2^T \, \mathbf{u}_3^T \, \mathbf{u}_4^T \right]^T , \\ \mathbf{u}_j^T = \left[\begin{array}{ccccccc} \overset{0}{x}_1 & \overset{0}{x}_2 & \overset{0}{x}_3 & \omega_1 & \omega_2 & \omega_3 & \lambda \end{array} \right]_j , j = 1,2,3,4 \end{gathered} \tag{46}$$

the finite element formulation now involves eleven free parameters, which can be arranged similar to (46) to a column vector :

$$\boldsymbol{\alpha} = \left[\alpha_1, \alpha_2, \cdots, \alpha_{11} \right]^T . \tag{47}$$

For the sequel it is suitable to summarize the strain-displacement relations for the compatible and incompatible strains in matrix notation. The corresponding result being of the form :

$$\delta \mathbf{E}^c = \mathbf{B}_V \delta \mathbf{u} \; , \; \delta \mathbf{E}^{inc} = \mathbf{G}_V \delta \boldsymbol{\alpha} \; , \; \Delta \delta \mathbf{E}^c = \Delta \mathbf{u}^T \mathbf{B}_{VL}^T \delta \mathbf{u} . \tag{48}$$

Inserting the above equations into (32) the following matrix equation is obtained :

$$\left[\begin{array}{cc} \mathbf{K}_T & \mathbf{K}_E^T \\ \mathbf{K}_E & \mathbf{K}_{EE} \end{array} \right] \left[\begin{array}{c} \Delta \mathbf{u} \\ \Delta \boldsymbol{\alpha} \end{array} \right] = \left[\begin{array}{c} \mathbf{f}_{ext} \\ 0 \end{array} \right] - \left[\begin{array}{c} \mathbf{f}_{int}^c \\ \mathbf{f}_{int}^{inc} \end{array} \right] , \tag{49}$$

with

$$\mathbf{K}_T = \int_{\mathcal{B}} \mathbf{B}_V^T \mathbf{C} \, \mathbf{B}_L dV + \int_{\mathcal{B}} \mathbf{S}^T \mathbf{B}_{VL} dV , \tag{50}$$

$$\mathbf{K}_E = \int_{\mathcal{B}} \mathbf{B}_V^T \mathbf{C} \, \mathbf{G}_L dV , \quad \mathbf{K}_{EE} = \int_{\mathcal{B}} \mathbf{G}_V^T \mathbf{C} \, \mathbf{G}_L dV . \tag{51}$$

Since $\mathbf{B}_V = \mathbf{B}_L$, $\mathbf{G}_V = \mathbf{G}_L$ and $\mathbf{B}_{VL} = \mathbf{B}_{LV}$ all related matrices are symmetric. The integrations over the shell volume are to be carried out numerically after the well known procedure (Bathe (1996)) setting :

$$dV = \sqrt{G} d\theta^3 d\xi d\eta . \tag{52}$$

Since the parameters $\boldsymbol{\alpha}$ need not to satisfy interelement compatibility conditions their elimination at the element level is suitable. After condensation equation (49) reduces to :

$$(\mathbf{K}_T - \mathbf{K}_E^T \mathbf{K}_{EE}^{-1} \mathbf{K}_E) \Delta \mathbf{u} = \mathbf{K}_E^T \mathbf{K}_{EE}^{-1} \mathbf{f}_{int}^{inc} - \mathbf{f}_{int}^c + \mathbf{f}_{ext} , \tag{53}$$

which can be put into short form : $\tilde{\mathbf{K}}_T \Delta \mathbf{u} = \tilde{\mathbf{f}}$. After each iteration step the incompatible degrees of freedom have to be updated according to

$$\boldsymbol{\alpha}^{n+1} = \boldsymbol{\alpha}^n - \mathbf{K}_{EE}^{-1\,n} \mathbf{K}_E{}^n \Delta \mathbf{u} - \mathbf{K}_{EE}^{-1\,n} \mathbf{f}_{int}^{inc\,n} . \tag{54}$$

5.4 Transformation into a local basis

Table 4 : Flow chart of the finite element program.

- first iteration step ?
  - yes : initialize $\mathbf{d}$ and $\mathbf{d}_{,\alpha}$
    initialize $\boldsymbol{\alpha}$
  - no : read last $\mathbf{d}$ and $\mathbf{d}_{,\alpha}$
    read last $\boldsymbol{\alpha}$, $\mathbf{K}_{EE}^{-1}$, $\mathbf{K}_E$, $\mathbf{f}_{int}^{inc}$ and update $\boldsymbol{\alpha}$
- rotate $\mathbf{d}$ and $\mathbf{d}_{,\alpha}$
- loop over $n1$ gausspoints over ξ
  - loop over $n2$ gausspoints over η
    - compute the compatible strains $\delta \mathbf{E}^c$ and $\Delta \delta \mathbf{E}^c$
    - loop over $n3$ gausspoints over θ^3
      - compute the incompatible strains $\delta \mathbf{E}^{inc}$
      - compute the material tensor $\mathbf{C}$
      - compute the internal stresses $\mathbf{S}$
      - compute and add up $\mathbf{K}_T$, $\mathbf{K}_E$, $\mathbf{K}_{EE}$, $\mathbf{f}_{int}^c$, $\mathbf{f}_{int}^{inc}$
    - ENDLOOP
  - ENDLOOP
- ENDLOOP
- invert $\mathbf{K}_{EE}$
- compute $\tilde{\mathbf{K}}_T$ and $\tilde{\mathbf{f}}$
- save $\mathbf{K}_{EE}^{-1}$, $\mathbf{K}_E$ and $\mathbf{f}_{int}^{inc}$
- regular point ?
  - yes : transform $\tilde{\mathbf{K}}_T$ and $\tilde{\mathbf{f}}$
    set stiffness K into diagonal entry of $\tilde{\mathbf{K}}_T$
    at the positions related to $\hat{\omega}^3$
    retransform $\tilde{\mathbf{K}}_T$ and $\tilde{\mathbf{f}}$
- save new $\mathbf{d}$ and $\mathbf{d}_{,\alpha}$

The above described finite element procedure holds for shells involving geometry intersections. If, however,

smooth shells or regular nodes of compound shells are considered a slight modification is necessary to prevent the singularity of the tangent stiffness matrix. For this purpose the rotational degrees of freedom are first transformed into the local basis $\mathbf{e}_i$:

$$\hat{\omega}^i = \boldsymbol{\omega}\cdot\mathbf{e}^i = \omega^k(\mathbf{i}_k\cdot\mathbf{e}^i) = \Gamma^i_{.k}\,\omega^k \tag{55}$$

defined in (25). Then this transformation is considered to replace the stiffness matrix by

$$\tilde{\mathbf{K}}_l = \overline{\boldsymbol{\Gamma}}\tilde{\mathbf{K}}_T\overline{\boldsymbol{\Gamma}}^T\ . \tag{56}$$

This in turn requires the construction of the hyper matrix $\overline{\boldsymbol{\Gamma}}$, which is given by

$$\boldsymbol{\Gamma} = \begin{bmatrix} \mathbf{e}_1^T \\ \mathbf{e}_2^T \\ \mathbf{e}_3^T \end{bmatrix} \qquad \overline{\boldsymbol{\Gamma}} = \begin{bmatrix} \mathbf{I} & \mathbf{0} & 0 & \dots \\ \mathbf{0} & \boldsymbol{\Gamma} & 0 & \dots \\ 0 & 0 & 1 & \dots \\ \vdots & \vdots & \vdots & \ddots \end{bmatrix}\ . \tag{57}$$

Next all rows and columns of $\tilde{\mathbf{K}}_l$ related to the local component $\hat{\omega}^3$ are to be set to zero in order to avoid possible coupling effects, although they should be actually zero by applying (24). Finally the diagonal entry associated with $\hat{\omega}^3$ is to be set to a value K, which can be arbitrarily selected in the numerical procedure. It has been observed, that the magnitude of K does not affect the solution.

A similar modification is to be performed also to the force vector according to :

$$\tilde{\mathbf{f}}_l = \overline{\boldsymbol{\Gamma}}\tilde{\mathbf{f}}\ , \tag{58}$$

subsequently setting the components of $\tilde{\mathbf{f}}_l$ related to $\hat{\omega}^3$ to zero. After this procedure the force vector and the stiffness matrix are transformed back by using the corresponding inverse relations to (56) and (58).

To give an overview over the discussed finite element formulation, the flow chart of the finite element program is summarized in Tab. 4.

6 Numerical examples

Now attention is given to some numerical examples in order to show the prediction capability of the derived finite element formulation. With the aim of systematic comparisons benchmark tests from literature or examples with given analytical solutions will be analysed.

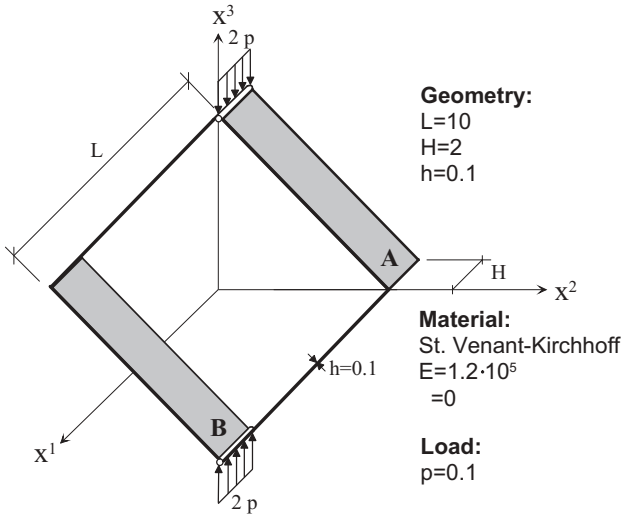

Figure 1 : Diamond shaped frame. Frame hinged at edge B, rigidly jointed at edge A and subjected to vertical line load p.

6.1 Large deflection of a diamond shaped frame

At first we consider a diamond shaped frame (Fig. 1), for which analytical solutions are given by (Jenkins, Seitz, and Przemieniecki (1966)) to assess the accuracy of the finite element results. In view of the symmetry of the structure we discretize only one half of the figure with a geometry intersection at edge A and a hinge at edge B using a $(10+10)\times 2$ mesh. The computation is performed with the kinematic assumption $A2$ given in Tab. 2. The computed results in steps of $\eta^2 = \lambda = 0.1$ are presented in Fig. 2. Note that η^2 is given as follows

$$\eta^2 = \frac{2(\lambda p)L^2}{EI} = \lambda \tag{59}$$

The results are in good agreement with the exact solution.

6.2 Pinched hemispherical shell with a circular hole

The hemispherical shell illustrated in Fig.3 is commonly regarded as a reliable benchmark to test the capability of the finite element formulation to deal with (nearly inextensible) bending dominated deformations. First a linear convergence analysis is performed through mesh refinement. Fig. 4 illustrates the results of the convergence analysis for the displacement X_A^1 and the displacement X_A^3 in dependence upon the element number per side. The result obtained for the vertical displacement $X_A^1 = 0.9343$ with a 32×32-mesh agrees well with the exact solution

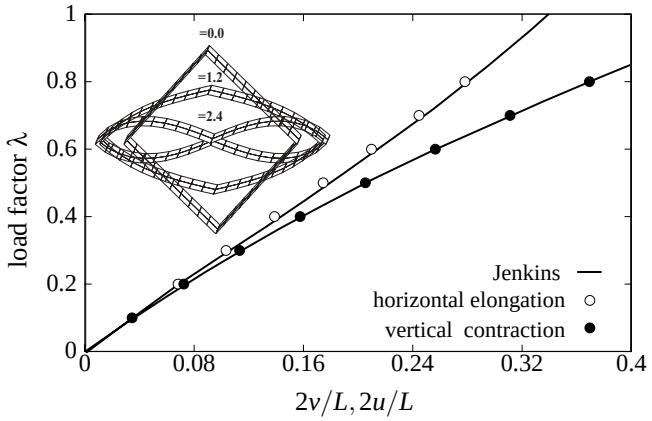

Figure 2 : Load factor-displacement diagram for horizontal elongation $2u/L$ at A and vertical contraction $2v/L$ at B.

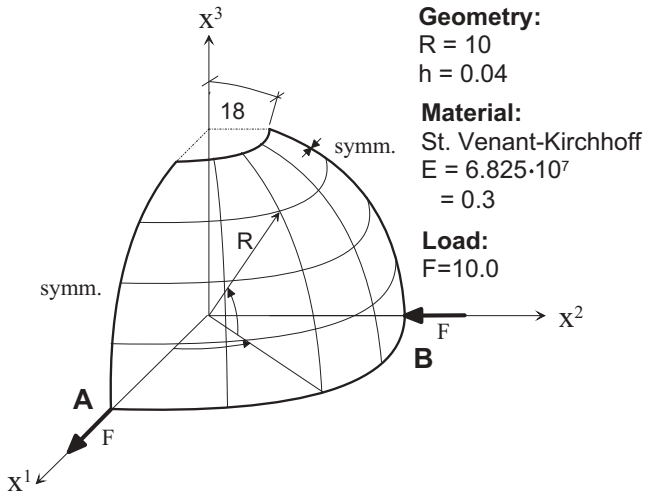

Figure 3 : Pinched hemispherical shell.

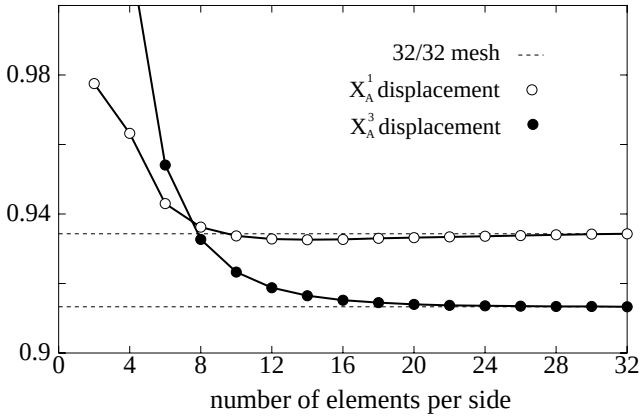

Figure 4 : Convergence analysis for the linear load step.

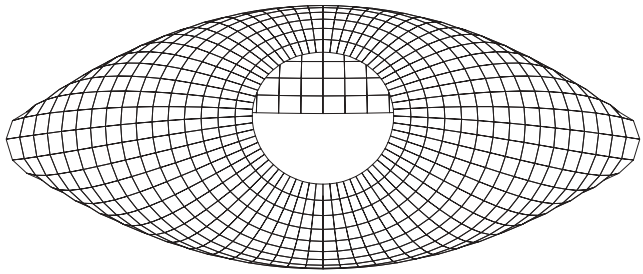

Figure 5 : Deformed configuration at $\lambda = 20$.

Table 5 : Comparison of enhanced and unenhanced solutions.

16×16	without	$\overset{1}{E}{}^{inc}_{33}$	$\overset{0}{E}{}^{inc}_{\alpha\beta}$	both
X_A^1/X_B^2	0.9272	0.9303	0.9291	0.9327
X_A^1	3.8751	3.9687	3.9518	4.0449
X_B^2	-7.4652	-7.7934	-7.7508	-8.1058

$X^1_{Aref} = 0.94$ (Simo, Fox, and Rifai (1989)). To give an insight how the *enhanced-strain concept* improves the solution the results of the pure displacement model (without enhancement) are compared in Tab. 5 for the linear case ($\lambda = 1$) and nonlinear case ($\lambda = 20$) with those obtained with membrane or transversal strain enhancements. The last two rows in Tab. 5 contain results of the nonlinear analysis. It is observable that both enhancements for E_{33} and $E_{\alpha\beta}$ are indispensable to achieve an accurate solution. This example has also been analysed by using different kinematic assumptions summarized in Tab. 2 and 3. First note that the above discussed solutions refer to formulation *A*. If the version *B* from Tab. 3 is used in the analysis following results are obtained: $X^1_A = 0.9334$ in the linear case and $X^2_B = -8.0448$ and $X^1_A = 4.0276$ for the load factor $\lambda = 20$ with a 16×16-mesh. The comparison of the results with those involved in Tab. 5 (enhanced solution) shows discrepancies about 7.5 per thousand for the nonlinear case. The discrepancy for the linear case is insignificant (0.75 per thousand). Consequently, in this example a decision can not be reached about the superiority of the versions *A* and *B*. It has been shown that the consideration of $\Delta\delta\mathbf{d}$ (assumption *A*2) accelerates the iteration procedure considerably in contrast to assumption *A*1, where $\Delta\delta\mathbf{d} = 0$. This can be deduced from the number of iteration steps given in Tab. 6. An energy criterium with the convergence accu-

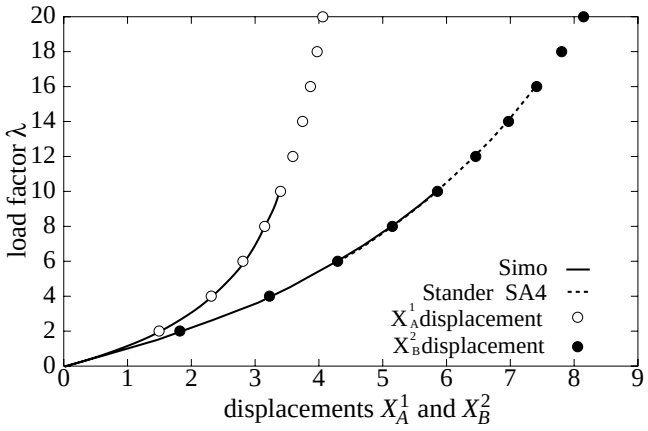

Figure 6 : Load-deformation plot of hemispherical shell.

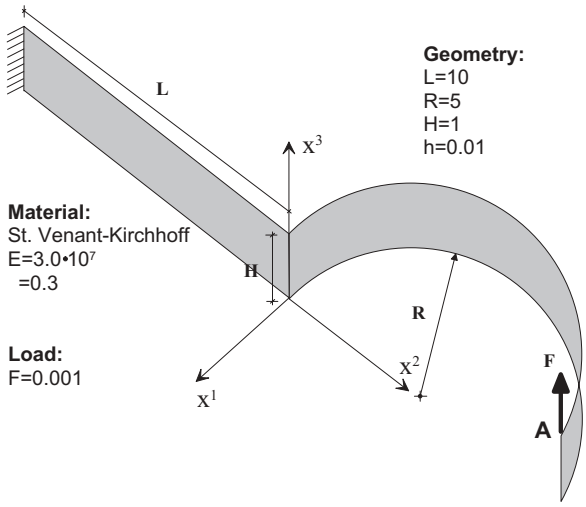

Figure 7 : Sickle shell problem.

racy level of 10^{-10} has been used for obtaining the results given there. Regarding the number of iteration steps the formulation *B* is practically equal to formulation *A*2. At the whole it should be pointed out that the consideration of the second order term $\Delta\delta\mathbf{d}$ is of major significance to save computational effort.

Table 6 : Number of iteration steps for ass. *A*1, *A*2 and *B*.

16×16	*A*1	*A*2	*B*
$\lambda=0\rightarrow\lambda=2$	12	11	11
$\lambda=18\rightarrow\lambda=20$	13	6	6

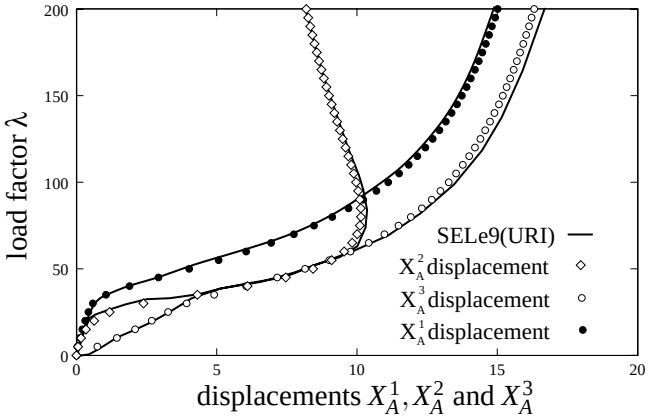

Figure 8 : Load-deformation plot of sickle shell.

The examination shows the good performance of the finite element formulation for kinematic assumption *A*2. This can be also confirmed by the plots given in Fig. 6 for the displacement, where for comparison also the results due to (Simo, Fox, and Rifai (1990)) for a 16×16-mesh and from STANDER for a 32×32-mesh (given in Chróścielewski, Makowski, and Stumpf (1997)) are illustrated. The solutions are in good agreement.

6.3 Sickle Shell problem

The next example, the sickle shell problem illustrated in Fig. 7, was proposed by SIMO (Simo (1993)). The linear solution $X_3^A=0.1499$ computed by the present element with a $(24+24)\times4$-mesh agrees very well with the exact solution $X_3^A=0.15$. In the cited article results are not given for the deep nonlinear range. However, in (Chróścielewski, Makowski, and Stumpf (1997)) results can be found until the load factor $\lambda=600$ computed with a 9-node degenerated shell element with uniform reduced integration(URI). The absolute values of the displacements at point A subjected to the force F by means of the *A*2-formulation with a $(24+24)\times4$-mesh are compared with the reference solutions for a $(10+10)\times2$-mesh in Fig. 8. The X_A^3-displacement slightly deviates from that obtained with the SELe9 element, but the displacements X_A^1 and X_A^2 are nearly identical.

6.4 Channel-section beam

The last example is a channel-section beam, which is illustrated in Fig. 10. From the examination of the hemispherical shell it could be concluded that the finite element works well for smooth shells. This example is suit-

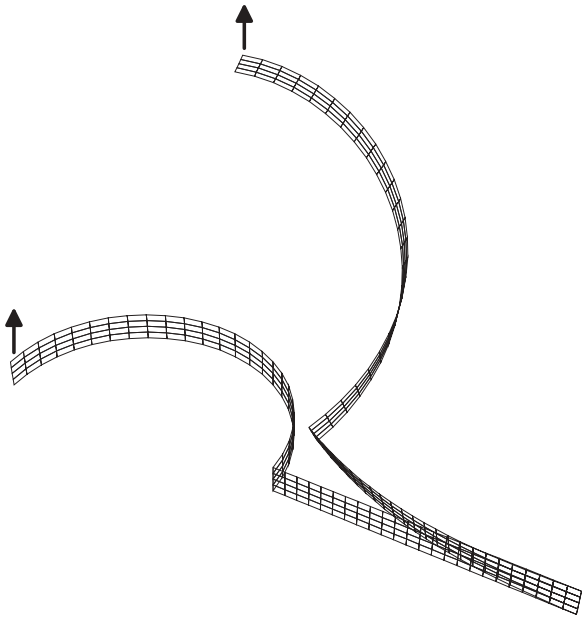

Figure 9 : Undeformed and deformed configuration ($\lambda = 50$).

Table 7 : Channel-section-beam: Linear solutions.

reference	mesh	displ. $w_A \times 10^{-3}$
Betsch	10×36	1.0998
Chróścielewski	CAM5 $\times$ 6e9	1.1373
rigid	10×36	1.1
without modif.	10×36	1.148

able to test the capability also for compound shells. The beam has two intersection lines. The intersection lines can be modelled rigidly by locking the seventh degree of freedom, the stretching parameter λ, at each node located at the intersection curves. By doing this we obtain the same solution as given in (Betsch, Gruttmann, and Stein (1996)) in the linear case. This has its cause in the similarity between both finite element formulations. We perform the computation solely for the $(2,6,2) \times 36$-mesh and compare the solutions with the results of the above cited reference and (Chróścielewski, Makowski, and Stumpf (1992)). In the last mentioned paper a 9 node Langrangian finite element has been used with a 5×6-mesh. In the first version we model the intersection lines rigidly in the way mentioned above. In the second version we make no modification. The nonlinear and linear results for $F = 1$ are compared with the above cited references in Fig. 12 and in Tab. 7.

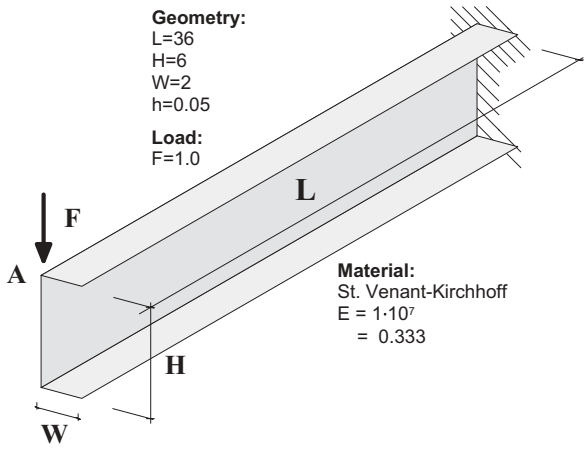

Figure 10 : Channel-section beam.

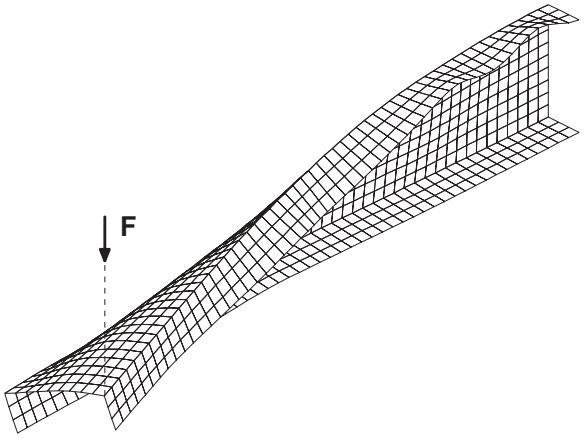

Figure 11 : Deformed structure at $w_A = 4.0$ for a 15×54-mesh.

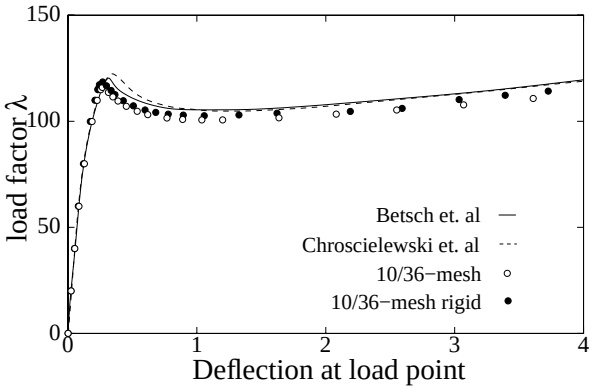

Figure 12 : Load-Deformation plot of channel-section beam.

7 Conclusion

In this contribution a four-node isoparametric finite element is proposed for large strain and finite rotation analysis of arbitrary shell structures. The original aspects of the development as distinct from the earlier derivations, cover

- the foundation of updated rotation procedure solely by the calculus of variation
- the consideration of second order variational terms for the determination of the director
- the inclusion of transverse strains and accordingly arbitrary three dimensional hyperelastic constitutive laws
- the consideration of single and compound shells in a unified approach

Due to the used *enhanced strain concept* membrane and POISSON´s locking effects are significantly reduced. The numerical procedure explained in Section 5.4 for regular nodes avoids effectively the singularity of the tangential stiffness matrix. The inclusion of second order variational terms accelerates the iterative procedure considerably.

But in any case the updated rotational procedure, although very effective in simulation of finite rotation, is and will remain as a variationally not consistent approach. The reason is that it does not define independent variational rotational quantities allowed to be directly interpolated. Accordingly the selection of interpolation polynomials can not follow to a well-defined procedure. Through the inclusion of several alternatives for this purpose it has been shown in this paper that this does not influence the reliability of the response, so that from a numerical point of view, it is at the whole not a weighty failure. The derivative of the current director is exactly evaluated at each node as follows :

$$
\begin{aligned}
\overset{n+1}{\mathbf{d}}_{,\alpha} =& -\sin(\omega)\,\omega_{,\alpha}\,\overset{n}{\mathbf{d}} + \cos(\omega)\,\overset{n}{\mathbf{d}}_{,\alpha} \\
&+ \frac{(\cos(\omega)\,\omega\,\omega_{,\alpha} - \sin(\omega)\,\omega_{,\alpha})}{\omega^2}\,\boldsymbol{\omega}\times\overset{n}{\mathbf{d}} \\
&+ \frac{\sin(\omega)}{\omega}\left(\boldsymbol{\omega}_{,\alpha}\times\overset{n}{\mathbf{d}} + \boldsymbol{\omega}\times\overset{n}{\mathbf{d}}_{,\alpha}\right) \\
&+ \frac{(\sin(\omega)\,\omega^2\,\omega_{,\alpha} - (1-\cos(\omega))\,2\,\omega\,\omega_{,\alpha})}{\omega^4}(\boldsymbol{\omega}\cdot\overset{n}{\mathbf{d}})\,\boldsymbol{\omega} \\
&+ \frac{1-\cos(\omega)}{\omega^2}((\boldsymbol{\omega}\cdot\overset{n}{\mathbf{d}})\,\boldsymbol{\omega}_{,\alpha} + (\boldsymbol{\omega}_{,\alpha}\cdot\overset{n}{\mathbf{d}})\,\boldsymbol{\omega} \\
&+ (\boldsymbol{\omega}\cdot\overset{n}{\mathbf{d}}_{,\alpha})\,\boldsymbol{\omega})\ .
\end{aligned}
\tag{60}
$$

with $\omega = \sqrt{\boldsymbol{\omega}\cdot\boldsymbol{\omega}}$ and $\omega_{,\alpha} = \frac{\boldsymbol{\omega}_{,\alpha}\cdot\boldsymbol{\omega}}{\omega}$ and

$$
\boldsymbol{\omega} = \sum_{L=1}^{4} N_L\,\boldsymbol{\omega}^L \qquad \boldsymbol{\omega}_{,\alpha} = \sum_{L=1}^{4} N_{L,\alpha}\,\boldsymbol{\omega}^L \tag{61}
$$

evaluated at the corresponding GAUSS-point.

References

Andelfinger, U.; Ramm, E. (1993): Eas-elements for two-dimensional, three-dimensional, plate and shell structures and their equivalence to hr-elements. *Int J Numer Methods Eng*, vol. 36, pp. 1311–1337.

Argyris, J.; Poterasu, V. F. (1993): Large rotations revisited application of lie algebra. *Comput Methods Appl Mech Eng*, vol. 103, pp. 11–42.

Atluri, S. N. (1984): Alternate stress and conjugate strain measures, and mixed variational formulations involving rigid rotations for computational analyses of finitely deformed plates and shells: Part i. theory. *Computers & Structures*, vol. 18, No. 1, pp. 93–116.

Atluri, S. N.; Cazzani (1995): Rotations in computational solid mechanics. *Archives for Computational Methods in Engg.*, vol. 2, No. 1, pp. 49–138.

Başar, Y.; Ding, Y. (1995): Interlaminar stress analysis of composites: layer-wise shell finite elements including transverse strains. *Composites Engineering*, vol. 5, No. 5, pp. 485–499.

Başar, Y.; Ding, Y.; Krätzig, W. B. (1992): Finite-rotation shell elements via mixed formulation. *Comput Mech*, vol. 10, No. 3/4, pp. 289–306.

Başar, Y.; Ding, Y.; Schultz, R. (1993): Refined shear-deformation models for composite laminates with finite rotations. *Int J Solids Struct*, vol. 30, pp. 2611–2638.

Başar, Y.; Itskov, M.; Eckstein, A. (2000): Composite laminates: Nonlinear interlaminar stress analysis by multi-layer shell elements. *Comput Methods Appl Mech Eng*, vol. 185, pp. 367–397.

Başar, Y.; Kintzel, O. (2000): Large rotation analysis of thin-walled shells. In Atluri, S. N.(Ed): *Advances in computational engineering and sciences, ICES´2K 20.-25. August 2000*, pp. 818–823. Tech Science Press.

Başar, Y.; Weichert, D. (2000): *Nonlinear continuum mechanics of solids*. Springer Berlin New York.

Bathe, K. J. (1996): *Finite element procedures*. Prentice-Hall International.

Bathe, K. J.; Dvorkin, E. N. (1985): Short communication a four-node plate bending element based on mindlin/reissner plate theory and a mixed interpolation. *Int J Numer Methods Eng*, vol. 21, pp. 367–383.

Betsch, P.; Gruttmann, F.; Stein, E. (1996): A 4-node finite shell element for the implementation of general hyperelastic 3d-elasticity at finite strains. *Comput Methods Appl Mech Eng*, vol. 130, pp. 57–79.

Bischoff, M.; Ramm, E. (1997): Shear deformable shell elements for large strains and rotations. *Int J Numer Methods Eng*, vol. 40, No. 23, pp. 4427–4449.

Brank, B.; Mamouri, S.; Ibrahimbegović, A. (2003): Constrained finite rotations in dynamics of shells and newmark implicit time-stepping schemes. *CMES: Comput Model Eng Sciences*, vol. 4, No. 1.

Büchter, N.; Ramm, E. (1992): Shell theory versus degeneration - a comparison in large rotation finite element analysis. *Int J Numer Methods Eng*, vol. 34, pp. 39–59.

Chróścielewski, J.; Makowski, J.; Stumpf, H. (1992): Genuinely resultant shell finite elements accounting for geometric and material non-linearity. *Inter J Num Methods Eng*, vol. 35, pp. 63–94.

Chróścielewski, J.; Makowski, J.; Stumpf, H. (1997): Finite element analysis of smooth, folded and multi-shell structures. *Comput Methods Appl Mech Eng*, vol. 141, pp. 1–46.

Harte, R.; Eckstein, U. (1986): Derivation of geometrically nonlinear finite elements via tensor notation. *Int J Numer Methods Eng*, vol. 23, pp. 367–384.

Iura, M.; Atluri, S. N. (1992): Formulation of a membrane finite element with drilling degrees of freedom. *Comput Mech*, vol. 9, pp. 417–428.

Jenkins, J. A.; Seitz, T. B.; Przemieniecki, J. S. (1966): Large deflections of diamond-shaped frames. *Int J Solids Struct*, vol. 2, pp. 591–603.

Nolte, L. P. (1983): Beitrag zur herleitung und vergleichende untersuchung geometrisch nichtlinearer schalentheorien unter berücksichtigung großer rotationen. Technical report, Mitteilung aus dem Institut für Mechanik. Nr. 39, Ruhr-Universität Bochum, 1983.

Parisch, H. (1991): An investigation of a finite rotation four node assumed strain shell element. *Int J Numer Methods Eng*, vol. 31, pp. 127–150.

Ramm, E. (1976): Geometrisch nichtlineare elastostatik und finite elemente. Technical report, Institut für Baustatik der Universität Stuttgart, Bericht Nr. 76-2, 1976.

Sansour, C.; Bufler, H. (1992): An exact finite rotation shell theory, its mixed variational formulation and its finite element implementation. *Int J Numer Methods Eng*, vol. 34, pp. 73–115.

Simo, J. C. (1993): On a stress resultant geometrically exact shell model. part 7: Shell intersections with 5/6-dof finite element formulations. *Comput Methods Appl Mech Eng*, vol. 108, pp. 319–339.

Simo, J. C.; Armero, F. (1992): Geometrically nonlinear enhanced strain mixed methods and the method of incompatible modes. *Int J Numer Methods Eng*, vol. 33, pp. 1413–1449.

Simo, J. C.; Fox, D. D. (1989): On a stress resultant geometrically exact shell model. part 1: Formulation and optimal parametrization. *Comput Methods Appl Mech Eng*, vol. 72, pp. 267–304.

Simo, J. C.; Fox, D. D.; Rifai, M. S. (1989): On a stress resultant geometrically exact shell model. part 2: The linear theory; computational aspects. *Comput Methods Appl Mech Eng*, vol. 73, pp. 53–92.

Simo, J. C.; Fox, D. D.; Rifai, M. S. (1990): On a stress resultant geometrically exact shell model. part 3: Computational aspects of the nonlinear theory. *Comput Methods Appl Mech Eng*, vol. 79, pp. 21–70.

Simo, J. C.; Rifai, M. S. (1990): A class of mixed assumed strain methods and the method of incompatible modes. *Int J Numer Methods Eng*, vol. 29, pp. 1595–1638.

Simo, J. C.; Rifai, M. S.; Fox, D. D. (1990): On a stress resultant geometrically exact shell model. part 4: Variable thickness shells with through-the-thickness stretching. *Comput Methods Appl Mech Eng*, vol. 81, pp. 91–126.

Suetake, Y.; Iura, M.; Atluri, S. N. (2003): Variational formulation and symmetric tangent operator for shells with finite rotation field. *CMES: Comput Model Eng Sciences*, vol. 4, No. 1.

Yeo, S. T.; Lee, B. C. (1996): Equivalence between enhanced assumed strain method and assumed hybrid method based on the hellinger-reissner principle. *Int J Numer Methods Eng*, vol. 39, pp. 3083–3099.